

# Role of the ferroelastic strain in the optical absorption of BiVO<sub>4</sub>

Cite as: APL Mater. **8**, 081108 (2020); <https://doi.org/10.1063/5.0011507>

Submitted: 21 April 2020 . Accepted: 20 July 2020 . Published Online: 18 August 2020

Christina Hill , Mads C. Weber , Jannis Lehmann , Tariq Leinen, Manfred Fiebig, Jens Kreisel, and Mael Guennou 




View Online



Export Citation

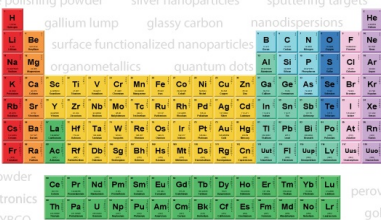


CrossMark



**AMERICAN ELEMENTS**

THE ADVANCED MATERIALS MANUFACTURER®



additive manufacturing   epitaxial crystal growth   cerium oxide polishing powder   silver nanoparticles   sputtering targets   III-IV semiconductors   CVD precursors   europium phosphors

gallium lump   glassy carbon   nanodispersions   InAs wafers   laser crystals   ultra high purity materials   MOFs

surface functionalized nanoparticles   organometallics   quantum dot   rare earth metals   photovoltaics   refractory metals   MOCVD

superconductors   transparent ceramics   ultra high purity silicon

*American Elements opens up a world of possibilities so you can **Now Invent!***

Over 15,000 certified high purity laboratory chemicals, metals, & advanced materials and a state-of-the-art Research Center. Printable GHS-compliant Safety Data Sheets. Thousands of new products. And much more. All on a secure multi-language "Mobile Responsive" platform.

perovskite crystals   yttrium iron garnet   alternative energy   h-BN

gold nanocubes   graphene oxide   macromolecules   photonics

rhodium sponge   fiber optics   beamsplitters   infrared dyes   zeolites

fused quartz   metallocenes   platinum ink   buckyballs   Ti-6Al-4V

deposition slugs   OLED Lighting   spintronics   solar energy

osmium   nanoribbons   thin films   chalcogenides   AuNPs

GDC   li-ion battery electrolytes   99.999% ruthenium spheres

endohedral fullerenes   copper nanoparticles   diamond micropowder

CIGS   MBE grade materials   palladium catalysts   flexible electronics

beta-barium borate   borosilicate glass   dysprosium pellets   YBCO

pyrolytic graphite   3d graphene foam   indium tin oxide   mesoporous silica

raman substrates   sapphire windows   tungsten carbide   InGaAs

barium fluoride   carbon nanotubes   lithium niobate   scandium powder

**Now Invent.™**

The Next Generation of Material Science Catalogs

[www.americanelements.com](http://www.americanelements.com)



# Role of the ferroelastic strain in the optical absorption of BiVO<sub>4</sub>

Cite as: APL Mater. 8, 081108 (2020); doi: 10.1063/5.0011507h

Submitted: 21 April 2020 • Accepted: 20 July 2020 •

Published Online: 18 August 2020



Christina Hill,<sup>1,2,a)</sup>  Mads C. Weber,<sup>3</sup>  Jannis Lehmann,<sup>3</sup>  Tariq Leinen,<sup>3</sup> Manfred Fiebig,<sup>3</sup> Jens Kreisel,<sup>2</sup> and Mael Guennou<sup>2</sup> 

## AFFILIATIONS

<sup>1</sup>Materials Research and Technology Department, Luxembourg Institute of Science and Technology, 41 rue du Brill, L-4422 Belvaux, Luxembourg

<sup>2</sup>Department of Physics and Materials Science, University of Luxembourg, 41 rue du Brill, L-4422 Belvaux, Luxembourg

<sup>3</sup>Department of Materials, ETH Zurich, Vladimir-Prelog-Weg 4, 8093 Zurich, Switzerland

<sup>a)</sup>Author to whom correspondence should be addressed: [christina.hill@list.lu](mailto:christina.hill@list.lu)

## ABSTRACT

Bismuth vanadate (BiVO<sub>4</sub>) has recently been under focus for its potential use in photocatalysis thanks to its well-suited absorption edge in the visible light range. Here, we characterize the optical absorption of a BiVO<sub>4</sub> single crystal as a function of temperature and polarization direction by reflectance and transmittance spectroscopy. The optical bandgap is found to be very sensitive to the temperature, and to the tetragonal-to-monoclinic ferroelastic transition at 523 K. The anisotropy, as measured by the difference in the absorption edge for the light polarized parallel and perpendicular to the principal axis, is reduced from 0.2 eV in the high-temperature tetragonal phase to 0.1 eV at ambient temperature. We show that this evolution is dominantly controlled by the ferroelastic shear strain. These findings provide a route for further optimization of bismuth vanadate-based light absorbers in photocatalytic devices.

© 2020 Author(s). All article content, except where otherwise noted, is licensed under a Creative Commons Attribution (CC BY) license (<http://creativecommons.org/licenses/by/4.0/>). <https://doi.org/10.1063/5.0011507h>

Bismuth vanadate (BiVO<sub>4</sub>) has recently attracted considerable attention for photocatalytic applications.<sup>1–4</sup> This is primarily due to its optical absorption properties in the visible range: the reported bandgap value<sup>5</sup> of 2.5 eV is close to the optimal value<sup>6</sup> of 2.2 eV desired for an efficient use of the solar spectrum. The position of the valence band edge of BiVO<sub>4</sub> is also well suited for efficient band-alignment for photoanodes in water splitting devices.<sup>7</sup> Besides, bismuth vanadate exhibits high chemical- and photo-stability in aqueous electrolytes,<sup>8</sup> and hence does not require a protective layer. To fully understand and optimize the behavior of BiVO<sub>4</sub> as a photoabsorber, a detailed understanding of its electronic and optical properties is highly desirable. This task, however, is relatively complex compared to classical semiconducting materials, due to the chemical complexity of BiVO<sub>4</sub>, its optical anisotropy, and its polymorphism.

BiVO<sub>4</sub> has three common crystal forms whose accessibility depends on the synthesis method:<sup>9</sup> the zircon structure with a tetragonal symmetry and two scheelite structures with the

monoclinic and tetragonal symmetry.<sup>9,10</sup> It is known that only the monoclinic scheelite BiVO<sub>4</sub> possesses optical properties suitable for applications in photocatalysis.<sup>11</sup> In its scheelite structure, BiVO<sub>4</sub> exhibits a reversible second-order ferroelastic phase transition at  $T_c = 523 \pm 5$  K from a high-temperature tetragonal symmetry (space group I4<sub>1</sub>/a) to a low-temperature monoclinic symmetry [space group I2/a – C2/c (15) in the standard setting].<sup>12–15</sup> This phase transition is driven by a spontaneous shear strain developed in the plane perpendicular to the tetragonal axis; it was studied in detail in the past as a rather uncommon example of a proper ferroelastic transition.<sup>16–22</sup>

The electronic and optical properties of scheelite BiVO<sub>4</sub>, in contrast, have been under focus much more recently, and are still under discussion. While the value of the bandgap, around 2.5 eV, is agreed on, its nature remains controversial. On the one hand, several experimental works report a direct bandgap.<sup>23–25</sup> On the other hand, most density functional theory (DFT) studies conclude that the bandgap is indirect, but also predict a direct

transition only a few hundreds of meV above the indirect bandgap.<sup>10,26</sup> This scenario is difficult to confirm by classical methods, such as optical spectroscopy or ellipsometry. Only recently, Cooper *et al.* confirmed by resonant inelastic X-ray scattering that the fundamental bandgap is indeed indirect with a direct band-to-band transition only 200 meV above it.<sup>5</sup> In addition, early single crystal studies have reported strong changes in color with varying temperatures.<sup>21</sup> This raises important questions on whether the direct and the indirect transition show the same temperature dependence, and how reliable the comparison of the experimental room temperature data with 0 K-DFT calculations is. Finally, because of the anisotropic structure of scheelite BiVO<sub>4</sub>, dichroism is expected and has indeed been predicted by several groups through DFT calculations<sup>10,26,27</sup> but has not been confirmed experimentally.

Here, we address these questions by a linear spectroscopy study of scheelite BiVO<sub>4</sub> single crystals as a function of temperature. We quantify the thermochromic behavior and the anisotropy of the optical absorption and show that it is sensitive to the ferroelastic phase transition. Specifically, we show that, in the monoclinic phase, the shift of the absorption edge is dominated by the ferroelastic shear strain.

Two samples were cut and polished from a larger single crystal pulled by the Czochralski-method. Figure 1(a) shows the tetragonal unit cell of scheelite BiVO<sub>4</sub>; all forthcoming indications of orientations are given with respect to this tetragonal unit cell. Note that the tetragonal 4-fold axis becomes the monoclinic 2-fold axis, and thus remains the principal axis in both phases. The first sample has a (110) surface orientation and a thickness of 360 μm; the second sample has a (001)-oriented surface and a thickness of 100 μm, see Figs. 1(b) and 1(c). The transmittance and reflectance measurements were performed with a Jasco MSV-370 microspectrophotometer. The spectrophotometer operates a deuterium lamp for the UV and a halogen lamp for the visible and near infrared light range and collects the light using non-dispersive Schwarzschild objectives. The

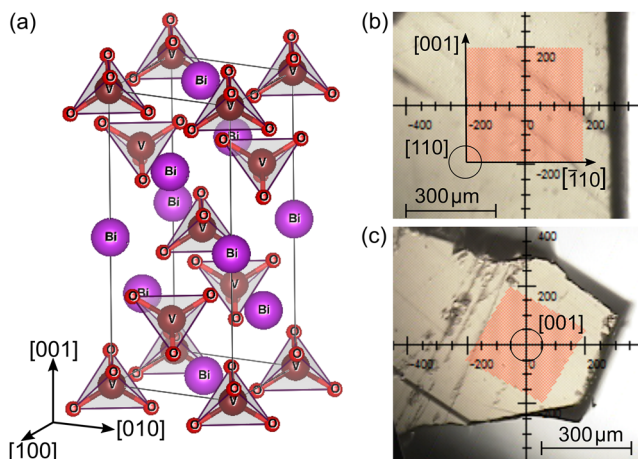


**FIG. 1.** (a) Schematic representation of the tetragonal unit cell of BiVO<sub>4</sub>. Optical microscopy images of (b) the (110)-oriented sample and (c) the (001)-oriented sample. For both samples, optical measurements were done with a vertical and a horizontal light polarization. The measurement areas are highlighted in red.

samples were placed in a Linkam THMS600 heating stage. Using an aperture, the measurement areas were set to 400 × 400 μm<sup>2</sup> and 300 × 300 μm<sup>2</sup> for the (110)-oriented sample and the (001)-oriented sample, respectively. In all cases, great care was taken to position the measurement area on the sample in homogeneous regions, i.e., free of domain walls or surface cracks. For all reflectance measurements, an aluminum mirror was used for calibration.

We first discuss the results for the (110)-oriented sample. Experiments were performed with two different directions of the linear light polarization  $P$ : first, with  $P$  parallel to the crystallographic axis [001] and second, with  $P \parallel [\bar{1}10]$ , see Fig. 1(b). The data are shown in Fig. 2. For both light polarization directions, reflectance and transmittance data show a pronounced temperature dependence, with an absorption edge shifting to longer wavelengths as temperature increases. To investigate the nature of the bandgap and its possible change with temperature, the absorption coefficient was calculated. In the spectral range of the fundamental absorption edge, the absorption coefficient  $\alpha$  is approximated by

$$\alpha = \frac{1}{t} \ln\left(\frac{1-R}{T}\right),$$

where  $T$  is the transmittance,  $R$  the reflectance, and  $t$  the sample thickness.<sup>28</sup> Figures 3(a) and 3(b) show the absorption coefficient vs temperature for both polarization directions. The theory of inter-band optical absorption reveals that the absorption coefficient  $\alpha$  varies with the photon energy according to the well-known relation  $(\alpha h\nu)^n = A(h\nu - E_{\text{opt}})$ , where  $A$  is a constant and  $E_{\text{opt}}$  is the optical

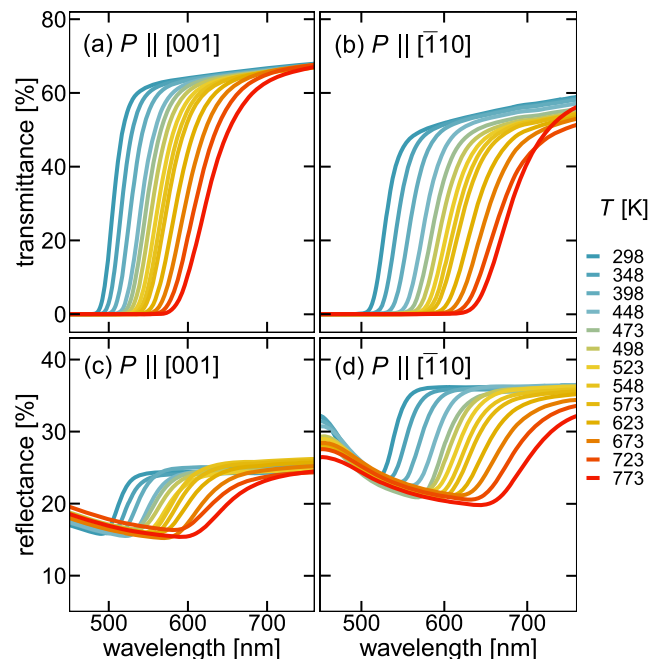


**FIG. 2.** Transmittance spectra measured on the (110)-oriented sample (a) for  $P \parallel [001]$  and (b) for  $P \parallel [\bar{1}10]$  as a function of temperature. (c) and (d) Reflectance spectra for  $P \parallel [001]$  and  $P \parallel [\bar{1}10]$ , respectively.

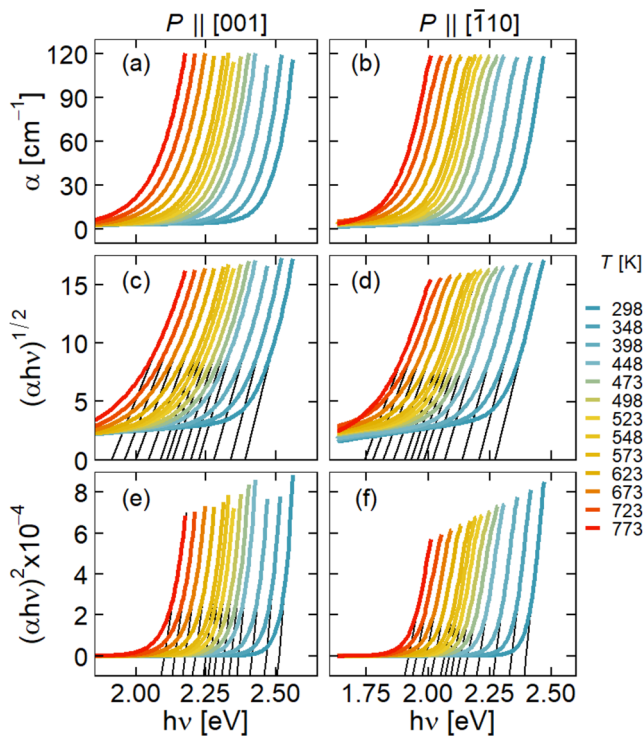


**FIG. 3.** [(a) and (b)] Optical absorption coefficient calculated from transmittance and reflectance data of the (110)-oriented sample for  $P \parallel [001]$  and  $P \parallel [110]$ , respectively. [(c) and (d)] and [(e) and (f)] Tauc plots calculated for both polarization directions, assuming an indirect and a direct bandgap, respectively.

absorption edge.<sup>29</sup> Here,  $n$  characterizes the nature of the transition process, which dominates the optical absorption. We have  $n = 2$  for a direct band-to-band transition and  $n = 0.5$  for an indirect band-to-band transition. Usually, the value of  $E_{\text{opt}}$  is determined by plotting  $(\alpha hv)^n$  vs the photon energy  $hv$  in a so-called Tauc plot. Hence, data are described by a straight line for  $n = 2$  in the case of a direct bandgap and for  $n = 0.5$  in the case of an indirect bandgap. This allows us to determine the nature of the bandgap.  $E_{\text{opt}}$  is given by the intercept of the linear fit with the photon-energy axis. Figures 3(c) and 3(d) show the Tauc plots for both light polarizations assuming indirect ( $n = 0.5$ ) and Figs. 3(e) and 3(f) for direct ( $n = 2$ ) transition. In all four cases, the data can be described by a straight line making it difficult to conclude on the nature of the transition with this measurement alone. Considering the similar curve shape of the absorption coefficient at each temperature, there are no indications that first, the nature of the transition differs from one to the other light polarization and second, the nature of the transition changes with temperature. Following the recent conclusions by Cooper *et al.* on the indirect nature of the bandgap, we extract an energy for the absorption edge of 2.27 eV for  $P \parallel [110]$  and of 2.39 eV for  $P \parallel [001]$  at room temperature.

In the next step, we investigated the anisotropy of the optical absorption. To analyze the data without having to rely on any particular hypothesis on the nature of the bandgap, we define the

absorption edge as the inflexion point of the transmittance curve. We determined this point by fitting the first derivative of the transmittance curve with an asymmetric Gaussian function. This function was chosen because it produces a satisfactory fit for all data and provides a consistent analysis, although we do not claim any particular physical meaning for it. The results are shown in Fig. 4. In first approximation, the evolution of the absorption edges was fitted linearly, with separate fits above and below  $T_c$ . Figure 4(a) shows the absorption edge obtained for the (110)-oriented sample for both polarizations. We notice that first, the absorption is clearly anisotropic in the tetragonal phase, with an energy difference of  $\approx 0.2$  eV between the two polarizations. This difference remains constant for temperatures above  $T_c$ , and the absorption edge decreases at the same rate of  $\approx -0.85$  meV  $K^{-1}$  for both light polarizations. Second, we observe a clear kink at  $T_c$  in the temperature evolution of the absorption edge for both light polarizations. Below  $T_c$ , in the monoclinic phase, the evolutions for both light polarizations remain linear, albeit with different slopes. This demonstrates that the absorption edge is sensitive to ferroelastic strain. These findings are robust even if alternative methods to extract the absorption edge are used. The corresponding plots are provided in the [supplementary material](#).

In the monoclinic phase, the optical absorption is expected to be anisotropic also in the plane perpendicular to the principal axis. To estimate the magnitude of this anisotropy, we performed a similar experiment with the (001)-oriented sample. We first measured

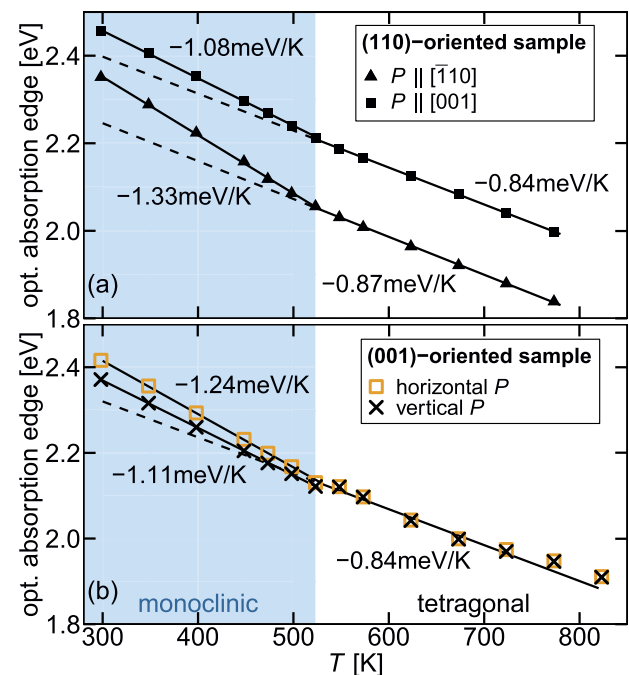


**FIG. 4.** Temperature dependence of the optical absorption edge for (a) the (110)-oriented sample and (b) the (001)-oriented sample. The solid lines are fits to the data. The dashed lines are extrapolations of the high-temperature trend into the low-temperature region.



the transmittance at room temperature, at a fixed wavelength of 515 nm, as a function of the polarization direction (see [supplementary material](#)). We then positioned the crystal in such a way that the extrema of this curve were found for vertical and horizontal light polarization [Fig. 1(c)], and proceeded to the measurements over the full wavelength range. The difference in absorption edges measured in this configuration amounts to 45 meV at room temperature. Transmittance spectra were also collected with increasing temperature, and the corresponding absorption edges are shown in Fig. 4(b). The energy difference decreases with increasing temperature and vanishes at  $T_c$ , as expected from the tetragonal symmetry. This should be considered as a first estimation, notably because we neglect here the effect of birefringence. A detailed study of the anisotropy in the monoclinic plane would require further experimental work. For the purpose of the present work, we simply observe that the anisotropy in this plane is comparatively small so that the fundamental bandgap is found for the light polarized perpendicular to the principal axis at room temperature and above.

Having established that the optical absorption is clearly sensitive to the ferroelastic transition, it is insightful to decompose the observed variations of the absorption edges as a function of the different components of strain. For that purpose, we use the detailed knowledge of the volume, lattice constants, and strains across the phase transition in Ref. 21, and focus here on the (110)-oriented sample. Figure 5(a) shows the evolution of the unit-cell volume across the phase transition and the corresponding thermal expansion coefficients. In the high-symmetry tetragonal phase, only

thermal expansion is present and both absorption edges follow linear and parallel evolutions at an average rate of  $\approx -0.85$  meV  $K^{-1}$  for a volumetric thermal expansion coefficient of  $\approx 4.7 \times 10^{-5} K^{-1}$  (details of the calculations are provided in the [supplementary material](#)). At the transition, the volume exhibits a kink and the thermal expansion is reduced to  $1.4 \times 10^{-5} K^{-1}$  below  $T_c$ . Assuming the same scaling, this would account for a change in the absorption edge of  $\approx -0.25$  meV  $K^{-1}$ , which is only a small fraction of the total change shown in Fig. 4(a). We conclude that the ferroelastic shear strain dominates the evolution of the optical bandgap in the monoclinic phase. This spontaneous shear strain develops in the ( $ab$ ) plane, has  $B_g$  symmetry, and is the primary order parameter of the transition.<sup>21</sup> In Fig. 5(b), we show the temperature evolution of the total shear strain calculated from the  $a$ ,  $b$ , and  $\gamma$  lattice parameters as defined by Aizu<sup>30</sup> and reported in Ref. 21. The respective influences of volume vs shear strain to the optical absorption are best illustrated in Fig. 5(c), where we show the absorption edges vs the unit-cell volume. The contribution of the simple volume change in the monoclinic phase is shown by the extrapolated dashed line and is clearly marginal. In the inset of Fig. 5(c), we also show the difference in optical bandgap  $\Delta E$  caused by the phase transition as a function of temperature for both polarizations. In both cases, the evolution deviates from linearity, which again is an indication that they scale predominantly with the shear strain.<sup>21</sup>

Finally, we discuss our observations in the light of the current theoretical understanding of the optical absorption in scheelite  $\text{BiVO}_4$ .<sup>10,26,27,31</sup> Our experimental observations, as described above with our tentative Tauc plots, are consistent with the facts given in the introduction, at all temperatures up to 773 K. We confirm the strong anisotropy of the optical absorption. At all temperatures, and irrespective of the anisotropy in the (001)-plane, the lowest absorption edge is found when the light is polarized perpendicular to the principal axis. For a quantitative comparison of the bandgap value(s) and the anisotropy, one should bear in mind the strong temperature dependence, and therefore extrapolate the experimental values down to 0 K. This extrapolation is not trivial because the behavior at low temperatures is non-linear for various reasons: the strain dependence described above, and a possible saturation of the order parameter at low temperatures,<sup>32</sup> and also the usual non-linear lattice anharmonicity and electron-phonon interactions.<sup>33</sup> The first effect can be taken into account by fitting a power law  $\Delta E_{\text{opt}} = A(T_c - T)^\beta$  to the data below  $T_c$ —this yields an extrapolated value of 2.62 eV at 0 K. Saturation of the order parameter in  $\text{BiVO}_4$  can be neglected, as demonstrated by birefringence studies.<sup>34</sup> On the other hand, the other non-linear effects cannot be neglected *a priori*. In the [supplementary material](#), we use physical arguments to show that they could lead to an additional lowering of the extrapolated value by as much as  $\approx 0.3$  eV. In any case, the experimental value agrees well with the calculated value of 2.47 eV from Ref. 10. On the other hand, we find a significant difference in the magnitude of the anisotropy between the light polarized parallel and perpendicular to the principal axis; because of the influence of the shear strain, the difference between absorption edges is reduced to 90 meV at 0 K, which is much weaker than the theoretical value<sup>10</sup> of 0.5 eV. In light of the sensitivity to shear strain described above, we hypothesize that these disagreements find their origin in the accuracy with which the calculation captures the small monoclinic distortion of the scheelite structure. Better quantitative

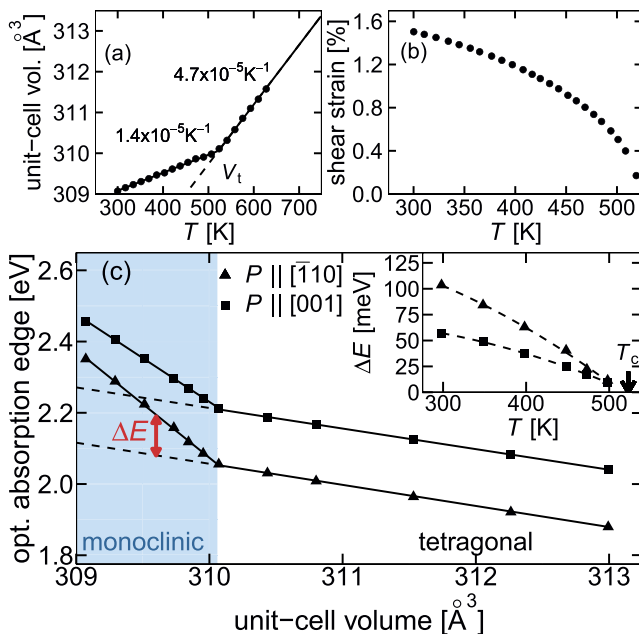


**FIG. 5.** (a) Evolution of the unit-cell volume across the phase transition and (b) of the shear strain in the monoclinic phase, as discussed in the text. Data are taken from Ref. 21. (c) Absorption edge for  $P \parallel [001]$  and  $P \parallel [\bar{1}10]$  as a function of the unit-cell volume. Inset: Difference in absorption edges  $\Delta E$  associated with the phase transition as a function of temperature.

predictions may require a particular attention to these structural aspects.

In summary, the optical absorption in scheelite bismuth vanadate has been measured over a wide temperature range, and the importance of its ferroelastic transition has clearly been established. The bandgap of 2.27 eV extracted at room temperature is in good agreement with the bandgap values published previously. While our data do not directly provide conclusive support for the indirect nature of the bandgap, they do show that its nature remains unchanged in the investigated temperature range. We find that the high-symmetry tetragonal phase exhibits a constant anisotropy in optical absorption of 0.2 eV, depending on whether the light is polarized parallel or perpendicular to the principal axis. The fundamental bandgap was found for the light polarized perpendicular to the principal axis, consistent with the expectations from DFT calculations, pointing to the possibility to activate different band-to-band transitions by playing with the polarization of the light. We show that the position of the absorption edge of bismuth vanadate is very sensitive to the onset of the spontaneous shear strain that develops in the low-symmetry phase, dominates the evolution, and enhances the thermochromic behavior. These results suggest that the optimization of the optical properties of BiVO<sub>4</sub>-based light absorbers would benefit from a careful control of the crystallite orientation. The sensitivity to strain could also be exploited via interface effects, epitaxy, nano-size effects, or cation substitution.

See the [supplementary material](#) for a description of alternative methods to extract the absorption edge from optical spectra, details on the positioning of the (001)-oriented sample, details on the calculation of the thermal expansion, and a discussion of the non-linear evolution of the absorption edge at low temperatures.

C.H. acknowledges funding from the Fond National de la Recherche under Project No. PRIDE/15/10935404. M.F. and J.L. acknowledge support by the ETH Grant No. ETH-28 14-1. M.F. and M.C.W. are grateful for financial support from the SNSF (Grant No. 200021\_178825). The authors also gratefully acknowledge M. Glazer (University of Oxford) for discussions and valuable insights into early studies of BiVO<sub>4</sub> single crystals.

## DATA AVAILABILITY

The data that support the findings of this study are openly available in Zenodo at <https://doi.org/10.5281/zenodo.3967205>.

## REFERENCES

- <sup>1</sup>F. F. Abdi, L. Han, A. H. M. Smets, M. Zeman, B. Dam, and R. van de Krol, "Efficient solar water splitting by enhanced charge separation in a bismuth vanadate-silicon tandem photoelectrode," *Nat. Commun.* **4**, 2195 (2013).
- <sup>2</sup>P. Bornoz, F. F. Abdi, S. D. Tilley, B. Dam, R. van de Krol, M. Graetzel, and K. Sivula, "A bismuth vanadate-cuprous oxide tandem cell for overall solar water splitting," *J. Phys. Chem. C* **118**, 16959 (2014).
- <sup>3</sup>L. Chen, E. Alarcón-Lladó, M. Hettick, I. D. Sharp, Y. Lin, A. Javey, and J. W. Ager, "Reactive sputtering of bismuth vanadate photoanodes for solar water splitting," *J. Phys. Chem. C* **117**, 21635 (2013).
- <sup>4</sup>L. Han, F. F. Abdi, R. van de Krol, R. Liu, Z. Huang, H.-J. Lewerenz, B. Dam, M. Zeman, and A. H. M. Smets, "Efficient water-splitting device based on a bismuth vanadate photoanode and thin-film silicon solar cells," *ChemSusChem* **7**, 2832 (2014).
- <sup>5</sup>J. K. Cooper, S. Gul, F. M. Toma, L. Chen, Y.-S. Liu, J. Guo, J. W. Ager, J. Yano, and I. D. Sharp, "Indirect bandgap and optical properties of monoclinic bismuth vanadate," *J. Phys. Chem. C* **119**, 2969 (2015).
- <sup>6</sup>A. Walsh, Y. Yan, M. N. Huda, M. M. Al-Jassim, and S.-H. Wei, "Band edge electronic structure of BiVO<sub>4</sub>: Elucidating the role of the Bi s and V d orbitals," *Chem. Mater.* **21**, 547 (2009).
- <sup>7</sup>Y. Park, K. J. McDonald, and K.-S. Choi, "Progress in bismuth vanadate photoanodes for use in solar water oxidation," *Chem. Soc. Rev.* **42**, 2321 (2013).
- <sup>8</sup>S. Chu, W. Li, Y. Yan, T. Hamann, I. Shih, D. Wang, and Z. Mi, "Roadmap on solar water splitting: Current status and future prospects," *Nano Futures* **1**, 022001 (2017).
- <sup>9</sup>S. Tokunaga, H. Kato, and A. Kudo, "Selective preparation of monoclinic and tetragonal BiVO<sub>4</sub> with scheelite structure and their photocatalytic properties," *Chem. Mater.* **13**, 4624 (2001).
- <sup>10</sup>T. Das, X. Rocquefelte, R. Laskowski, L. Lajaunie, S. Jobic, P. Blaha, and K. Schwarz, "Investigation of the optical and excitonic properties of the visible light-driven photocatalytic BiVO<sub>4</sub> material," *Chem. Mater.* **29**, 3380 (2017).
- <sup>11</sup>X. Zhang, Z. Ai, F. Jia, L. Zhang, X. Fan, and Z. Zou, "Selective synthesis and visible-light photocatalytic activities of BiVO<sub>4</sub> with different crystalline phases," *Mater. Chem. Phys.* **103**, 162 (2007).
- <sup>12</sup>J. Bierlein and A. Sleight, "Ferroelasticity in BiVO<sub>4</sub>," *Solid State Commun.* **16**, 69 (1975).
- <sup>13</sup>W. I. F. David, A. M. Glazer, and A. W. Hewat, "The structure and ferroelastic phase transition of BiVO<sub>4</sub>," *Phase Transitions* **1**, 155 (1979).
- <sup>14</sup>A. Sleight, H.-y. Chen, A. Ferretti, and D. Cox, "Crystal growth and structure of BiVO<sub>4</sub>," *Mater. Res. Bull.* **14**, 1571 (1979).
- <sup>15</sup>J. Pellicer-Porres, D. Vázquez-Socorro, S. López-Moreno, A. Muñoz, P. Rodríguez-Hernández, D. Martínez-García, S. N. Achary, A. J. E. Rettie, and C. B. Mullins, "Phase transition systematics in BiVO<sub>4</sub> by means of high-pressure-high-temperature Raman experiments," *Phys. Rev. B* **98**, 214109 (2018).
- <sup>16</sup>G. Benyuan, M. Copic, and H. Z. Cummins, "Soft acoustic mode in ferroelastic BiVO<sub>4</sub>," *Phys. Rev. B* **24**, 4098 (1981).
- <sup>17</sup>R. M. Hazen and J. W. E. Mariathasan, "Bismuth vanadate: A high-pressure, high-temperature crystallographic study of the ferroelastic-paraelastic transition," *Science* **216**, 991 (1982).
- <sup>18</sup>I. G. Wood, B. Welber, W. I. F. David, and A. M. Glazer, "Ferroelastic phase transition in BiVO<sub>4</sub> II. Birefringence at simultaneous high pressure and temperature," *J. Appl. Crystallogr.* **13**, 224 (1980).
- <sup>19</sup>W. I. F. David, "Ferroelastic phase transition in BiVO<sub>4</sub>: III. Thermodynamics," *J. Phys. C: Solid State Phys.* **16**, 5093 (1983).
- <sup>20</sup>W. I. F. David, "Ferroelastic phase transition in BiVO<sub>4</sub>: IV. Relationships between spontaneous strain and acoustic properties," *J. Phys. C: Solid State Phys.* **16**, 5119 (1983).
- <sup>21</sup>W. I. F. David and I. G. Wood, "Ferroelastic phase transition in BiVO<sub>4</sub>: V. Temperature dependence of Bi<sup>3+</sup> displacement and spontaneous strains," *J. Phys. C: Solid State Phys.* **16**, 5127 (1983).
- <sup>22</sup>H. Cummins and A. Levanyuk, in *Light Scattering Near Phase Transitions, Modern Problems in Condensed Matter Sciences* (Elsevier Science, 1983).
- <sup>23</sup>S. Stoughton, M. Showak, Q. Mao, P. Koirala, D. A. Hillsberry, S. Sallis, L. F. Kourkoutis, K. Nguyen, L. F. J. Piper, D. A. Tenne, N. J. Podraza, D. A. Muller, C. Adamo, and D. G. Schlom, "Adsorption-controlled growth of BiVO<sub>4</sub> by molecular-beam epitaxy," *APL Mater.* **1**, 042112 (2013).
- <sup>24</sup>H. Luo, A. H. Mueller, T. M. McCleskey, A. K. Burrell, E. Bauer, and Q. X. Jia, "Structural and photoelectrochemical properties of BiVO<sub>4</sub> thin films," *J. Phys. Chem. C* **112**, 6099 (2008).
- <sup>25</sup>B. Zhou, J. Qu, X. Zhao, and H. Liu, "Fabrication and photoelectrocatalytic properties of nanocrystalline monoclinic BiVO<sub>4</sub> thin-film electrode," *J. Environ. Sci.* **23**, 151 (2011).
- <sup>26</sup>Z. Zhao, Z. Li, and Z. Zou, "Electronic structure and optical properties of monoclinic clinobisvanite BiVO<sub>4</sub>," *Phys. Chem. Chem. Phys.* **13**, 4746 (2011).
- <sup>27</sup>K. Ding, B. Chen, Z. Fang, and Y. Zhang, "Density functional theory study on the electronic and optical properties of three crystalline phases of BiVO<sub>4</sub>," *Theor. Chem. Acc.* **132**, 1352 (2013).

- <sup>28</sup>F. Demichelis, G. Kaniadakis, A. Tagliaferro, and E. Tresso, "New approach to optical analysis of absorbing thin solid films," *Appl. Opt.* **26**, 1737 (1987).
- <sup>29</sup>J. I. Pankove, *Optical Processes in Semiconductors* (Dover, New York, 1975).
- <sup>30</sup>K. Aizu, "Determination of the state parameters and formulation of spontaneous strain for ferroelastics," *J. Phys. Soc. Jpn.* **28**, 706 (1970).
- <sup>31</sup>N. Wadnerkar and N. J. English, "Density functional theory investigations of bismuth vanadate: Effect of hybrid functionals," *Comput. Mater. Sci.* **74**, 33 (2013).
- <sup>32</sup>E. K. H. Salje, B. Wruck, and H. Thomas, "Order-parameter saturation and low-temperature extension of Landau theory," *Z. Phys. B: Condens. Matter* **82**, 399 (1991).
- <sup>33</sup>I. A. Vainshtein, A. F. Zatsepin, and V. S. Kortov, "Applicability of the empirical Varshni relation for the temperature dependence of the width of the band gap," *Phys. Solid State* **41**, 905 (1999).
- <sup>34</sup>I. G. Wood, "Spontaneous birefringence of ferroelastic BiVO<sub>4</sub> and LaNbO<sub>4</sub> between 10 K and  $T_c$ ," *J. Phys. C: Solid State Phys.* **17**, L539 (1984).